

<https://helda.helsinki.fi>

Fast imaging-based single particle analysis method for solubility determination

Hokkala, Emma

2022-08-25

Hokkala , E , Strachan , C J , Agopov , M , Semjonov , K , Heinämäki , J , Yliruusi , J & Svanback , S 2022 , ' Fast imaging-based single particle analysis method for solubility determination ' , International Journal of Pharmaceutics , vol. 624 , 121976 . <https://doi.org/10.1016/j.ijpharm.2022.121976>

<http://hdl.handle.net/10138/351007>

<https://doi.org/10.1016/j.ijpharm.2022.121976>

cc_by

publishedVersion

Downloaded from Helda, University of Helsinki institutional repository.

This is an electronic reprint of the original article.

This reprint may differ from the original in pagination and typographic detail.

Please cite the original version.



Fast imaging-based single particle analysis method for solubility determination

Emma Hokkala^{a,*}, Clare J. Strachan^a, Mikael Agopov^b, Kristian Semjonov^c, Jyrki Heinämäki^c, Jouko Yliruusi^b, Sami Svanbäck^b

^a Division of Pharmaceutical Chemistry and Technology, Faculty of Pharmacy, University of Helsinki, Viikinkaari 5 E, 00790 Helsinki, Finland

^b The Solubility Company, Viikinkaari 4, 00790 Helsinki, Finland

^c Institute of Pharmacy, Faculty of Medicine, University of Tartu, Nooruse 1, 50411 Tartu, Estonia

ARTICLE INFO

Keywords:

Solubility
Dissolution
Single particle
Optical imaging
Image analysis
Miniaturization

ABSTRACT

The solubility and dissolution rates of chemical compounds are crucial properties in several fields of industry and research. However, accurate, rapid and green methods for their measurement, which only consume micrograms of compound, are lacking. Here, the unique approach of non-specific, image-based single particle analysis (SPA) for solubility testing is directly compared to and thus validated on the mid-solubility range with the current gold standard shake-flask method with UV-Vis spectroscopy employed for determining sample concentrations. Five biologically active compounds representing a range of physicochemical properties including pK_a and $\log P$ were analyzed with both methods. The comparison of SPA and the shake-flask (SF) analysis shows excellent linear correlation ($R^2 = 0.99$). Higher variability of the SPA method is attributed to variability between the properties of individual particles, which cannot be detected with traditional methods. Due to the similar average solubility values compared to those produced with SF, it is concluded that the SPA method has great potential as an analytical tool for small-scale solubility studies. It also has several practical advantages over the current gold standard shake-flask method, such as speed, low consumables consumption, and no requirement for prior knowledge of compound chemistry.

1. Introduction

Solubility (S) of any given compound plays an important role in diverse fields of industry, including the chemical, environmental, food and cosmetic industries. In the pharmaceutical industry, solubility and dissolution rate are crucial characteristics of all active pharmaceutical ingredients, as they affect drug discovery and development, and ultimately the behavior of the drug in the body (Di et al., 2012). In terms of efficacy, even the most potent drug will not have any effect, if it cannot dissolve in the body.

Organic solvents, both those deemed green and environmentally problematic (Tobiszewski et al., 2017), are not only needed in synthesizing and purifying the drug compound, but also in the manufacturing and formulation processes, analyses of the drug compound and formulation, and in some cases, in the end-product itself. In addition to aqueous solvents also being utilized in the aforementioned processes, biorelevant aqueous solvents are used to estimate the drug's behavior in

the GI tract. Therefore, knowing the solubility of a compound in these solvents is essential for process and formulation development and optimization. Moreover, being able to determine the solubility with as little material consumption as possible helps with energy and waste management. Such techniques could also help with development and establishment of alternative, greener solvents (Prat et al., 2016), gradually taking the industry towards international environmental goals.

There are several methods to determine the solubility of compounds, with the focuses in this article being equilibrium solubility (maximum concentration of a compound in a certain solvent at a certain temperature and pressure) and apparent solubility (temporary solubility of a thermodynamically metastable or unstable solid form) (Sugano et al., 2007). Current methods have several shortcomings, including expensive equipment usually used for a single purpose, long experimental times, method development, and multiple experimental and sampling steps, all resulting in high energy and material consumption.

For equilibrium solubility studies, the shake-flask (SF) method is

Abbreviations: SPA, Single particle analysis.

* Corresponding author.

E-mail address: emma.hokkala@helsinki.fi (E. Hokkala).

<https://doi.org/10.1016/j.ijpharm.2022.121976>

Received 11 April 2022; Received in revised form 24 June 2022; Accepted 30 June 2022

Available online 2 July 2022

0378-5173/© 2022 The Authors. Published by Elsevier B.V. This is an open access article under the CC BY license (<http://creativecommons.org/licenses/by/4.0/>).

considered the gold standard (Baka et al., 2008). In this method, an excess of compound is added to a solvent, and after a fixed period of shaking, usually at least 24 h, the concentration of dissolved drug is determined using e.g. UV spectrometry or HPLC. To reduce the high material consumption, several miniaturized equilibrium solubility methods based on the shake-flask method have been developed (Alyunas et al., 2009). For example, potentiometric methods, including the dissolution titration template (DTT), involve adding a weakly acidic compound to an acidic solvent (or a weakly basic compound to a basic solvent), and adding a titrant until the compound is completely dissolved (Avdeef and Berger, 2001). The Chasing equilibrium method, on the other hand, begins with a solution with the compound completely dissolved, to which a titrant is added until equilibrium solubility is found (Stuart and Box, 2005).

Kinetic solubility is usually studied by adding dimethyl sulfoxide (DMSO) stock solution to a buffer and measuring precipitation by e.g. UV absorbance (Lipinski et al., 2012). Other techniques for measuring precipitation are nephelometry, in which the intensity of radiation scattering from a sample is measured, and turbidimetry, in which the decrease in radiation intensity through a sample is determined (Morais et al., 2006).

An advantage of the shake-flask method is its reproducibility, with a reported mean standard deviation (SD) of 0.17–0.39 log units (Avdeef, 2015). However, it requires experimental times of hours to several days, relatively large amounts of solvent, compound consumption ranges from milligrams to grams, and determining concentrations require compound-specific analytical methods and calibration curves. Therefore, compound and solvent consumption, and operational costs are further increased. Furthermore, compound instability in solution, in addition to possible adsorption to the vial, cap or filter can lead to inaccurate results. Several experimental and sampling steps also lead to discarding of multiple consumables as hazardous waste including pipette tips, and depending on the throughput level, well plates and plate filters, or syringes and syringe filters.

The potentiometric DTT and the Chasing equilibrium methods are significantly faster and have been reported to have reproducibility of 0.36 and 0.52 log units, respectively (Avdeef, 2015), which is below the likely reproducibility of 0.6 log units (Jorgensen and Duffy, 2002). The DTT potentiometric method is approximately 10 times faster than the shake-flask method with minimal material consumption, in the range of 50–100 µg (Avdeef and Berger, 2001). The Chasing equilibrium procedure takes 20 to 80 min with a minimal material consumption of 2–5 mg (Stuart and Box, 2005). However, these methods are only suitable for ionizable compounds with pK_as of between 2 and 12, which account for 77.5 % of the World Health Organization Model List of Essential Medicines (Manalack, 2007). In addition, compound instability in solution and during titration remains an issue.

The kinetic solubility methods, on the other hand, are fast and allow for high-throughput measurement, but do not represent the equilibrium solubility values (Lipinski et al., 2012). In addition, all of the crystal lattice input in the solubility of the compound is lost when dissolved in DMSO. However, in drug discovery, the degree of crystallinity may be very different for newly synthesized compounds compared to compounds in the later stages of drug development (Gardner et al., 2004). Therefore, equilibrium solubility values cannot be obtained during early drug discovery. Even when the purity and crystallinity of the compounds improve, the number of drug candidates remains high. Thus, high-throughput equilibrium solubility studies are needed for both informed lead selection and optimal dosage form development. Thus far, such methods are lacking.

To address these environmental and other shortcomings, *in silico* solubility prediction methods have been investigated, but remain hampered by a high error, with a standard deviation of up to 1 log unit (Jorgensen and Duffy, 2002), which is largely due to a lack of high-quality experimental training datasets covering a diverse enough chemical space (Faller and Ertl, 2007). An additional problem is the

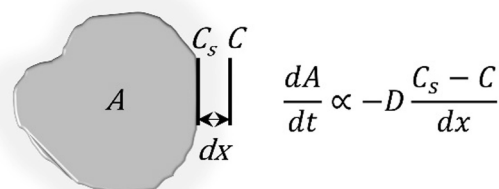


Fig. 1. The diffusion layer around a particle. The rate of decrease in area of the particle, dA/dt , depends on the diffusivity, D , of the compound, the concentration difference, $C_s - C$, between the solid–liquid interphase, C_s , and the bulk solvent, C , and the diffusion distance, x , as described by Fick's first law.

number and accuracy of computed molecular descriptors, such as octanol–water partition coefficient and polar surface area. Despite the high energy consumption of super computers, computational methods for predicting solubility are very environmentally friendly relative to chemical techniques. In addition to no material consumption, they have tremendous potential to save time and money in drug development, but as long as they cannot reach acceptable levels of error, other techniques are needed.

Optical imaging-based single particle analysis (SPA) has the potential to meet the current unmet environmental and practical needs of solubility studies. Originally developed by Svanbäck et al. (2015a, 2015b, 2014), this microscale method involves the acquisition of images of dissolving individual particles and converting the change in particle 2D morphology into dissolution data through image analysis. The SPA method is based on the diffusion layer theory, in which a stagnant liquid layer of saturated solution is assumed to exist around the dissolving particle (Higuchi, 1967; Noyes and Whitney, 1897). An equilibrium exists at the solid–liquid interface, and the rate of diffusion through the diffusion layer depends on the concentration difference across the diffusion layer. The SPA method keeps the dissolution environment under sink conditions, i.e., frequently transporting the dissolved compound away from the particle. Therefore, the solubility of the compound in the dissolution medium becomes the dissolution rate-limiting factor. Only the change in particle morphology as a function of time is considered, and thus the decrease in particle area may be related to mass transfer during dissolution as follows: the change in area, dA , as a function of time, dt , may be considered proportional to Fick's first law of diffusion (Fick, 1855), as the diffusion across the diffusion layer depends on the diffusivity, D , the concentration gradient, $C_s - C$, between the solid–liquid interphase, C_s , and the bulk solvent, C , as well as the diffusion distance, x , as shown in Fig. 1.

Due to the physical nature of optical imaging, no prior knowledge of the compound's chemistry is needed, and laborious chemical compound-specific analytical methods need not be developed. Highly sensitive image analysis with a lateral spatial detection limit of roughly 1 µm enables samples in the microgram range even for highly soluble compounds. Due to the small sample sizes, solvent consumption is also reduced to the milliliter range. In general, small-scale studies also reduce energy consumption, operational costs and time. Lack of sampling removes several steps in the experimental procedure, thus minimizing sources of error and saving time in addition to further reducing the number of consumables and labware used.

The aim of this work is to investigate the reliability of the SPA method in comparison to the gold standard shake-flask. Benefits of the SPA method listed above, coupled with accurate solubility data, would help informed decision-making regarding solubility, and by extension, e.g. lead selection and optimization for further development in pharmaceutical industry. In this regard, the SPA method has the potential to reduce costs in addition to material and energy consumption associated with drug development, making it a potential contributor to green pharmacy and by extension, to other industries benefitting from

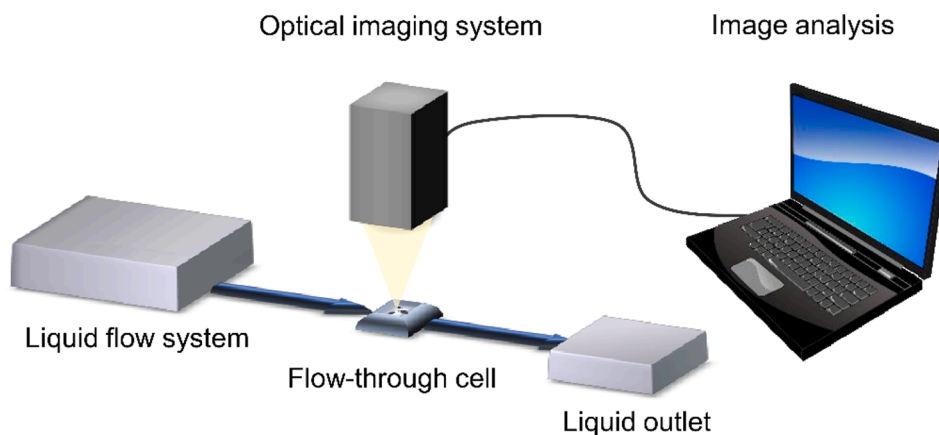


Fig. 2. The SPA configuration. The dissolution medium flows into the flow-through cell, where the particles are immobilized. Images of the dissolving individual particles are analyzed using a custom-developed algorithm.

solubility data, to green chemistry.

2. Materials and methods

2.1. Materials

Acetazolamide, sulfathiazole and theobromine were of analytical grade (Sigma-Aldrich CHEMIE GmbH, Germany). Acetaminophen and valsartan met USP testing specifications and pharmaceutical secondary standards, respectively (Sigma-Aldrich Co., USA). The drug compounds were used without further processing. Dulbecco's phosphate buffer saline (DPBS) pH 7.4 was the physiologically relevant dissolution medium (Sigma-Aldrich Co., USA). Prior to use, the DPBS concentrate was diluted 1:9 with MilliQ water (Millipore Integral 15, filtered with 0.22 μm Millipak Express filters). The pH was measured with a FieldLab pH meter (SCHOTT, Germany) and adjusted with 1 M HCl solution (VWR International S.A.S., France).

2.2. Characterization

2.2.1. X-ray powder diffractometry (XRPD)

The polymorphic forms of the commercially obtained drug compounds, both before the shake-flask experiments, and then after the shake-flask experiments and subsequent drying at ambient conditions, were analyzed with XRPD. Using sample sizes of approximately 5 mg, the XRPD diffractograms of rotating samples were collected in transmission mode with PanAnalytical Empyrean diffractometer (PanAnalytical, Netherlands), operated with Data Collector software (PanAnalytical, Netherlands). The XRPD involved $\text{CuK}\alpha$ radiation $\lambda = 1.5406 \text{ \AA}$ and was operated at 45 kV and 40 mA. Data was collected in θ - θ geometry in the range of 5° – 40° 2θ , with a step size of 0.0131303° and a total counting time of 159.120 s per step using the PIXcel3D detector with Medipix3 technology.

2.2.2. Scanning electron microscope (SEM)

SEM samples were prepared by fixing the drug powder on two-sided carbon adhesive on aluminum stubs and coated with a 5 nm layer of platinum in a Q150T turbo-pumped sputter coater (Quorum Technologies, UK). SEM images were taken with a Quanta 250 FEG SEM (FEI Company, USA), in low vacuum mode to prevent charging of the drug crystals, using LFD detection, high voltage of 10.00 kV, pressure of 41 Pa, spot size of 4.0 and dwell time of 5 μs .

2.3. SPA method

With the SPA device, the dissolution medium is pumped at a constant

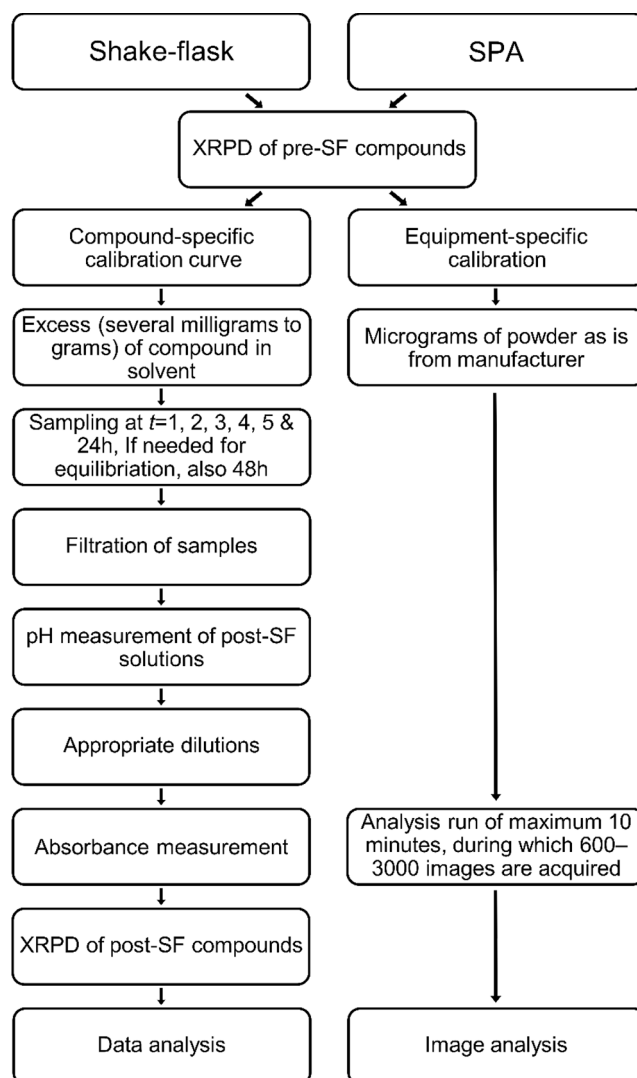


Fig. 3. Flow diagrams of the experimental protocols used in the present study. Pre-SF = pre-shake-flask experiments. Post-SF = post-shake-flask experiments.

flow rate through a custom-made flow-through cell, within which only micrograms of the dissolving drug particles are trapped. The dissolved molecules are constantly extracted from the flow-through cell,

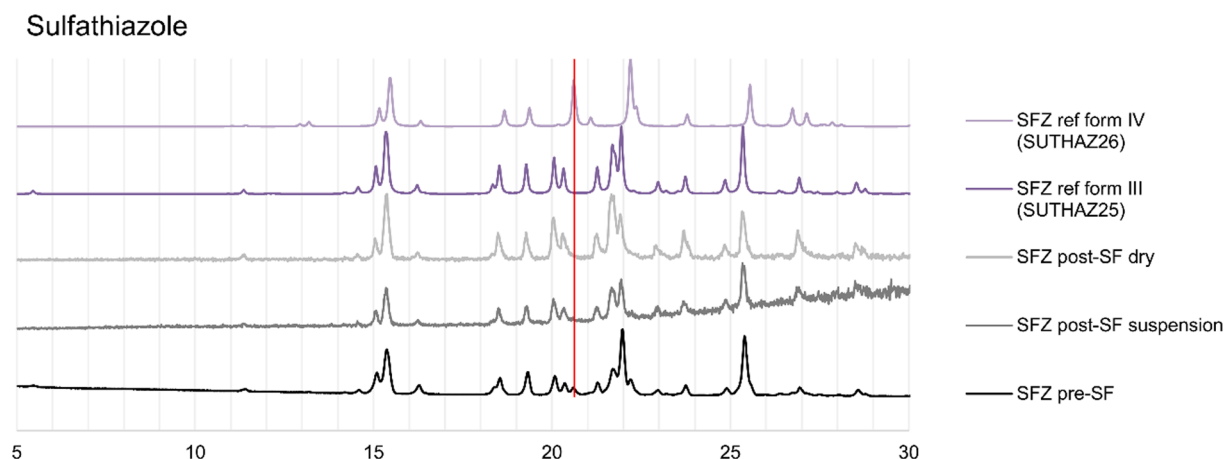


Fig. 4. XRPD diffractograms of the pre-SF metastable sulfathiazole (before shake-flask experiments, mixture of forms III and IV), the post-SF stable form III (analyzed after shake-flask experiments), and reference diffractograms from the Cambridge Structural Database (database identifier number in brackets). The red vertical line indicates the presence of form IV in the pre-SF sample, otherwise predominantly form III. (For interpretation of the references to colour in this figure legend, the reader is referred to the web version of this article.)

maintaining sink conditions in the cell. Images of the dissolving particles are taken with a digital camera. No sampling is required, reducing the number of experimental steps and thus sources of error. Image analysis is then performed on individual particles using a custom-developed algorithm (Matlab R2017a, version 9.2.0.538062, The MathWorks, Inc, USA). The algorithm transforms the change in particle morphology into dissolution data. The initial optimal particle size is approximately 10–100 μm with a detection limit of roughly 1 μm in diameter. The SPA configuration is illustrated in Fig. 2. The setup, calibration and image analysis are performed as described in previously published work (Stukelj et al., 2020, 2019a, 2019b; Svanbäck, 2016). The SPA method is validated on the low solubility range as explained in the work of Stukelj et al. (2019a), by comparing the intrinsic solubility values, *i.e.* solubility of unionized compounds, obtained with both SPA and SF methods. As the SPA method is physical in nature, the need for compound-specific calibration is eliminated, which further reduces operational costs and material consumption.

2.4. Shake-flask

Shake-flask samples were analyzed with a UV-1600PC spectrophotometer (VWR International bvba, Belgium) with accompanying software (M.Wave Professional v. 1.0.2, VWR International, USA), using compound-specific wavelengths. Calibration solutions were prepared by serially diluting DPBS stock solutions. Calibration curves ranged 5–50 $\mu\text{g}/\text{mL}$ except for theobromine, for which the calibration range was 1–10 $\mu\text{g}/\text{mL}$, and for valsartan, for which the range was 1.5–15 $\mu\text{g}/\text{mL}$. All of the calibration curves were linear with ten calibration points each and R^2 values ranging from 0.9994 to 0.9997.

The shake-flask experiments were performed in triplicate. An excess of compound was added to 10 mL of DPBS in glass vials, which were left

to shake at 21.5 ± 0.5 °C in a REAX 2 overhead shaker (Heidolph, Germany). Samples were taken at $t = 0, 1, 2, 3, 4, 5$ and 24 h. If needed for equilibration, samples were also taken at $t = 48$ h. The samples (375 μL) were filtered through 0.45 μm cellulose acetate syringe filters (VWR International, USA). The filtrates were diluted with DPBS until calibration range absorbances were reached. A flow-chart of the shake-flask protocol is presented in Fig. 3.

After the final sampling, the pH of the post-SF solutions was measured from the filtrates using a micro-pH electrode (WTW InoLab pH 7110, Xylem Analytics, Germany) before UV analysis. Excess DPBS was removed from the SF samples, and the suspensions were transferred to XRPD sample holders for diffractometer measurements. After the suspensions had dried, they were measured again to confirm the polymorphic form.

3. Results & discussion

3.1. Characterization

3.1.1. XRPD

Experimental diffractograms of the commercially obtained solid-state forms of the drug compounds were visually compared to XRPD reference patterns of known polymorphs from the Cambridge Structural Database (CSD). The thermodynamically stable polymorph was confirmed to be the commercial form for all compounds except sulfathiazole, which was a mixture of forms III and IV (Hu et al., 2013) that tend to crystallize together (Anwar et al., 1989), and for valsartan, which is marketed as an amorphous form (Wang et al., 2013). Thus, for these two compounds, the apparent solubility was initially studied as opposed to equilibrium solubility with the rest of the compound set.

The concentration values throughout the shake-flask experiments of

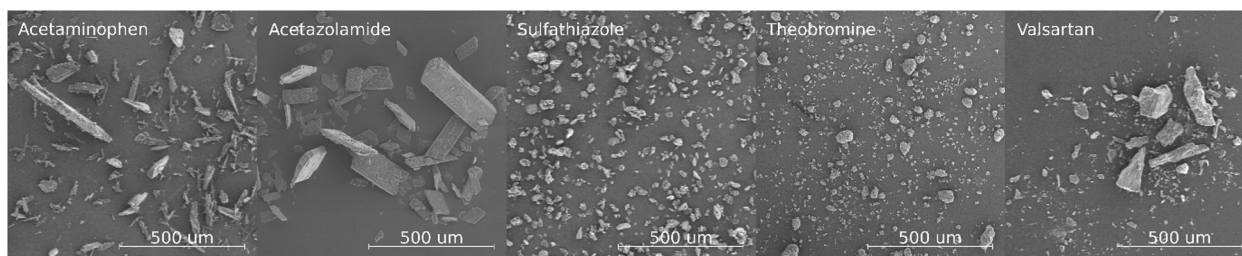


Fig. 5. SEM images of the compounds. The contrast and brightness of the SEM images were adjusted with Inkscape (Inkscape 0.92.5, The Inkscape Process) after image acquisition for a more uniform grayscale throughout images.

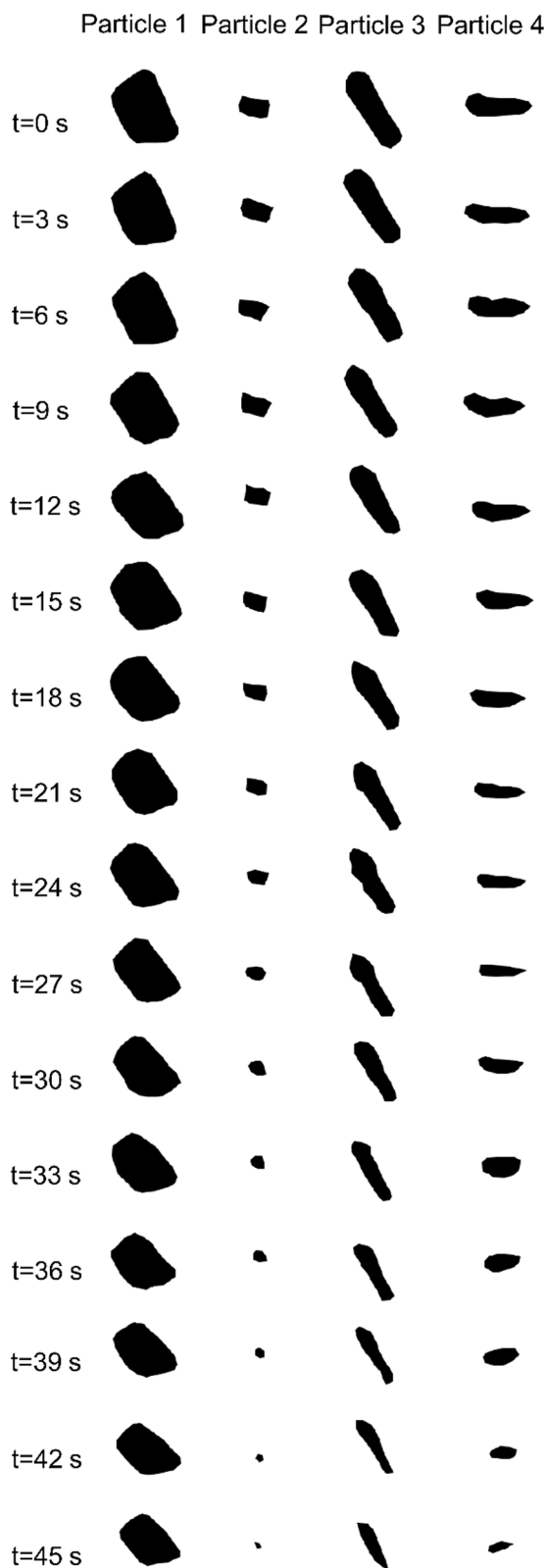


Fig. 6. Black and white 2D projection images of dissolving individual acetazolamide particles.

the metastable and unstable forms for sulfathiazole (SFZ) and valsartan (VLS), respectively, stayed constant throughout the experiments. A mixture of sulfathiazole forms III and IV tend to transition to form III in solution, which was confirmed with post-SF XRPD measurements (Fig. 4) (Munroe et al., 2012). The amorphous form of valsartan did not

crystallize during the 48 h its SF study lasted. Due to the lack of phase transformation, the obtained solubility value for VLS may be considered equilibrium solubility value in the current experimental timeframe (Sugano et al., 2007).

3.1.2. SEM

SEM images were taken to study particle size and morphologies of the drug compounds (Fig. 5). The compounds varied considerably in particle size, ranging from sulfathiazole particles of approximately 25–50 μm to acetazolamide particles of approximately 100–350 μm .

3.2. Dissolution of particles obtained with SPA

As an example of raw data gathered from a SPA measurement, black and white image series of four of the dissolving acetazolamide particles in the SPA system are shown in Fig. 6. An example of a dissolution curve (Fig. 7a), used to calculate solubility, is obtained with the Hixson-Crowell cube root equation (H-C) (Hixson and Crowell, 1931) [Equation (1)], assuming a spherical particle shape.

$$w_{max}^{1/3} - w_t^{1/3} = k_1 t \quad (1)$$

where w_{max} is the mass of the particle at $t = 0$, w_t is the mass at time t , and k_1 is the H-C rate constant. As the initial mass of the particle is not known, but the radius, r , is, the masses in Equation (1) are replaced with the respective particle radii at times $t = 0$ and t , based on the relationship between mass, density ρ and volume V in $w = \rho V = \rho(4/3)\pi r^3$, resulting in Equation (2),

$$r_{max} - r_t = k_2 t \quad (2)$$

where $k_2 = k_1 / \sqrt[3]{4/3\pi\rho}$. To calculate the relative dissolved amount using the equivalent sphere radius, Equation (2) transforms to:

$$\% \text{ Dissolved}(t) = \left(r_{max}^3 - r(t)^3 \right) / r_{max}^3 \quad (3)$$

When the particle became too small for accurate image analysis, the analysis was discontinued. Therefore, a particle size decrease until completion and thus 100% dissolution was extrapolated. A single particle solubility profile is shown in Fig. 7b, where it is seen that the solubility value equilibrated already after 3–5 s after starting the analysis.

3.3. Comparison of SPA and shake-flask values

The comparison between the SPA equilibrium solubility values and shake-flask values in log units is shown in Fig. 8. The linear correlation between the average solubility values was observed with the linear regression fit yielding an R^2 of 0.99. A significant difference between the lengths of the SPA error bars and the SF error bars can be seen, relating to the detection of properties of individual particles being investigated. Inherently, relative standard deviation is inversely proportional to the sample size. However, with the SPA method, the standard deviation does not reduce with increasing number of particles, as the variability is dependent on the properties of the individual particles: the more variability there is between the particles, the higher the standard deviation. The extremely sensitive image analysis detects differences in the solubility of the individual particles that look identical to the naked eye. With SPA, on average 15 individual particles per compound were studied, resulting in 15 individual solubility values per compound with a repeatability value of 0.22 log units.

For SF, on the other hand, in a single vial there are thousands of particles dissolving, resulting in a mean solubility value for those thousands of particles, and when performed in triplicate, three individual solubility values per compound, with a standard deviation value of 0.07 log units.

The reported reproducibility of interlaboratory SF experiments ranges between 0.17 and 0.39 log units (Avdeef, 2015). Due to the SPA

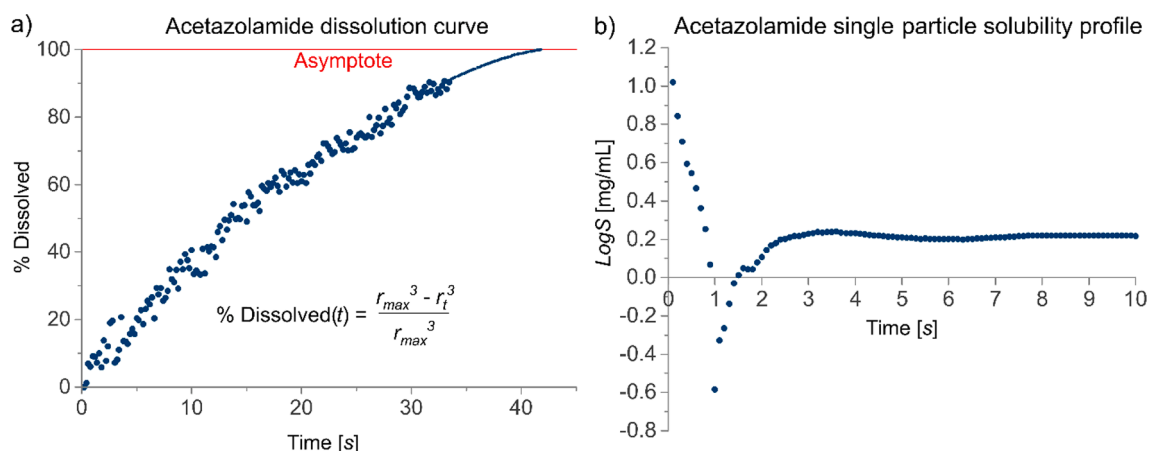


Fig. 7. a) Example of an acetazolamide dissolution curve, obtained with the Hixson-Crowell cube root equation using equivalent sphere radii, used to calculate solubility. When the particle became too small for accurate image analysis, analysis was discontinued and the rest of the curve was extrapolated. b) Example of a calculated acetazolamide solubility profile obtained from a single particle with a diameter of approximately 10 μm . The sample amount was in the nanogram range. It can be seen that solubility equilibrated already after 3–5 s. All graphs were plotted using OriginPro 2018 SR1 (v. b9.5.1.195, OriginLab Corporation, USA).

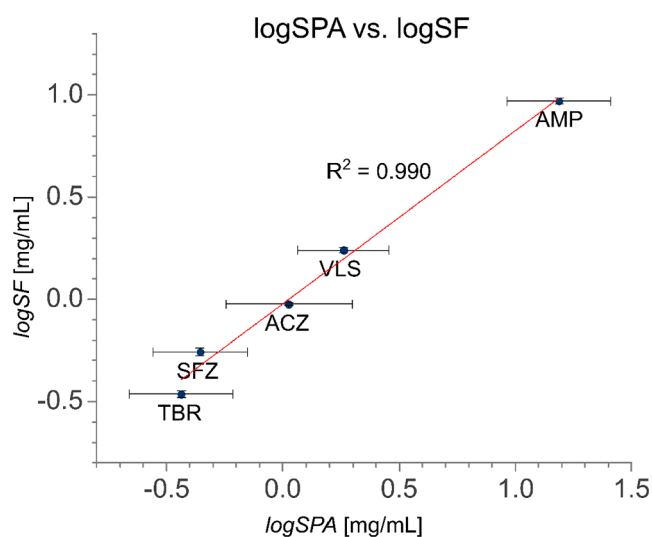


Fig. 8. Comparison between the SPA ($\log\text{SPA}$) and shake-flask ($\log\text{SF}$) values. ACZ = acetazolamide, AMP = acetaminophen, SFZ = sulfathiazole, TBR = theobromine, VLS = valsartan. Note that the error bars reflect the variance between individual particles from a single SPA measurement, and the variance between the averages of thousands of particles from three SF vials.

technology currently being used in a single laboratory, it is not possible to conduct complete reproducibility studies as per the ICH guideline (EMA, 1994), and therefore to properly compare the standard deviations between the two methods. Until that point, it can only be stated that the average solubility values obtained with the SF method and the SPA method are very similar.

The SPA solubility values are presented in Table 1 along with pK_a values and literature $\log\text{S}$ for commercial forms. In general, the literature values correlate well with the SPA values. Having said this, regarding experimental solubility values, different protocols, dissolution media, experimental temperatures, and polymorphic forms, for example, are all potential sources of large solubility differences. Even with the same protocols and solid-state forms, depending on e.g. the stability and relative complexity of the compound, solubility values can differ greatly (Avdeef, 2015; Kishi and Hashimoto, 1989). Due to these reasons, the reported literature values from several different sources with different protocols and experimental conditions are not optimal reference values, with the experimental values obtained in exactly the

Table 1

pK_a values, SPA solubility values, and experimental values for commercial forms obtained from the literature. Type of buffer (phosph = phosphate, citr = citrate) and its pH are in brackets, as is the temperature (RT = room temperature) if it has been mentioned in the reference. The average solubility values between the SPA and the SF methods correlate well.

Compound	pK_a value	SPA $\log\text{S}$ [mg/mL] values (DPBS pH 7.4)	SF $\log\text{S}$ [mg/mL] values (DPBS pH 7.4)	Literature aqueous $\log\text{S}$ [mg/mL] values
Acetazolamide	7.20 (O'Neil et al., 2013)	-0.0236	0.0261	0.0043 (phosph 6.85); 0.4456 (phosph 8.17, 25 °C) (Parasrampur and Das Gupta, 1990)
Acetaminophen	9.41 (Shalaeva et al., 2008)	0.9702	1.1884	1.1876 (phosph 7.4, 25 °C) (Baena et al., 2004)
Sulfathiazole	7.20 (O'Neil et al., 2013)	-0.2583	-0.3557	0.0043 (citr 7.38, 25 °C) (Higuchi et al., 1953)
Theobromine	10.05 (O'Neil et al., 2013)	-0.4640	-0.4368	-0.3010 (phosph 7.4, 37 °C) (Varshosaz and Falamarzian, 2001)
Valsartan	3.60, 4.70 (Tosco et al., 2008)	0.2401	0.2599	0.7340 (phosph-citr 6.8, 25 °C) (Huang et al., 2017)

same environment being more appropriate for comparison.

Considering the similar solubility values obtained with the SPA method and its practical advantages (Fig. 9), and subsequent environmental and cost advantages, when compared to the shake-flask method, this study suggests the SPA method is preferable to the current gold standard method.

4. Conclusions

We have shown that the SPA method, with numerous environmental and practical advantages, provides solubility values as reliable as the established gold standard shake-flask method. The SPA method



Shake-flask	vs.	SPA
		
5–100s mg	Sample size	1–10 µg
>24 h	Analysis time	10 min
Method development Calibration curves	Preparation	
Sampling Sample processing Analysis run Data analysis	Stages of analysis	Analysis run Data analysis

Fig. 9. Summary of experimental requirements for shake-flask and SPA methods.

consumes only micrograms of the drug compound and milliliters of solvent, and the analysis takes less than 10 min, compared to the shake-flask method that takes at least 24 h. With optical imaging, no *a priori* knowledge of the compound chemistry is needed, making the SPA method suitable for all compounds regardless of their chemistry, and abolishing the need for laborious chemical analyses and calibration development. Fewer process steps and the lack of sampling reduce the environmental impact of material and sampling device consumption and simplify the experimental procedure, with savings in time and a decrease in sources of error. Throughout the experimental procedure, material consumption and operational costs remain low. Overall, SPA produces similar solubility values as the SF method, with all the environmental and practical benefits of miniaturized image-based analysis. Thus, the unique SPA method has great potential for future solubility studies.

Chemical compounds studied in this article

Acetaminophen (PubChem CID 1983); Acetazolamide (PubChem CID 1986); Sulfathiazole (PubChem CID 5340); Theobromine (PubChem CID 5429); Valsartan (PubChem CID 60846).

CRedit authorship contribution statement

Emma Hokkala: Conceptualization, Methodology, Formal analysis, Investigation, Data curation, Writing – original draft, Visualization. **Clare J. Strachan:** Resources, Writing – review & editing, Supervision. **Mikael Agopov:** Software, Data curation. **Kristian Semjonov:** Investigation. **Jyrki Heinämäki:** Resources, Writing – review & editing. **Jouko Yliruusi:** Conceptualization, Methodology, Writing – review & editing, Supervision. **Sami Svanbäck:** Conceptualization, Methodology, Validation, Writing – review & editing, Supervision, Project administration, Funding acquisition.

Declaration of Competing Interest

The Solubility Company owns the intellectual property rights to the SPA method. E.H., M.A., J.Y., and S.S. are shareholders in The Solubility Company.

Data availability

The authors do not have permission to share data.

Acknowledgements

Business Finland, formerly the Finnish Funding Agency for Innovation (TEKES), is acknowledged for the funding of this project (award number 4511/31/2016). The Electron Microscopy Unit (EMBI) at the Institute of Biotechnology, University of Helsinki is acknowledged for

providing access to and help with SEM. Heikki Räikkönen at the University of Helsinki is thanked for helping with the XRPD measurements. The authors also acknowledge Mr. Jaan Aruväli and Prof. Kalle Kirsimäe from Department of Geography, Institute of Ecology and Earth Sciences, University of Tartu, Estonia, for their help with the XRPD measurements.

References

- Alelyunas, Y.W., Liu, R., Pelosi-Kilby, L., Shen, C., 2009. Application of a Dried-DMSO rapid throughput 24-h equilibrium solubility in advancing discovery candidates. *Eur. J. Pharm. Sci.* 37, 172–182. <https://doi.org/10.1016/j.ejps.2009.02.007>.
- Anwar, J., Tarling, S.E., Barnes, P., 1989. Polymorphism of Sulfathiazole. *J. Pharm. Sci.* 78, 337–342. <https://doi.org/10.1002/jps.2600780416>.
- Avdeef, A., 2015. Suggested improvements for measurement of equilibrium solubility-pH of ionizable drugs. *ADMET DMPK* 3, 84–109.
- Avdeef, A., Berger, C.M., 2001. pH-metric solubility. 3. Dissolution titration template method for solubility determination. *Eur. J. Pharm. Sci.* 14 (4), 281–291.
- Baena, Y., Pinzón, J.A., Barbosa, H.J., Martínez, F., 2004. Temperature-dependence of the solubility of some acetanilide derivatives in several organic and aqueous solvents. *Phys. Chem. Liq.* 42, 603–613. <https://doi.org/10.1080/00319100412331284413>.
- Baka, E., Comer, J.E.A., Takács-Novák, K., 2008. Study of equilibrium solubility measurement by saturation shake-flask method using hydrochlorothiazide as model compound. *J. Pharm. Biomed. Anal.* 46, 335–341. <https://doi.org/10.1016/j.jpba.2007.10.030>.
- Di, L., Fish, P.V., Mano, T., 2012. Bridging solubility between drug discovery and development. *Drug Discov. Today* 17, 486–495. <https://doi.org/10.1016/j.drudis.2011.11.007>.
- EMA, 1994. ICH Topic Q 2 (R1) Validation of Analytical Procedures: Text and Methodology. Step 5. Note for guidance on validation of analytical procedures: Text and methodology (CPMP/ICH/381/95), Prescrire International.
- Faller, B., Ertl, P., 2007. Computational approaches to determine drug solubility. *Adv. Drug Deliv. Rev.* 59, 533–545. <https://doi.org/10.1016/j.addr.2007.05.005>.
- Fick, A., 1855. Ueber Diffusion. *Ann. der Phys. und Chemie* 170, 59–86. <https://doi.org/10.1002/andp.18551700105>.
- Gardner, C.R., Walsh, C.T., Almarsson, Ö., 2004. Drugs as materials: valuing physical form in drug discovery. *Nat. Rev. Drug Discov.* 3, 926–934. <https://doi.org/10.1038/nrd1550>.
- Higuchi, T., Gupta, M., Busse, L.W., 1953. Influence of electrolytes, pH, and alcohol concentration on the solubilities of acidic drugs. *J. Am. Pharm. Assoc. (Scientific ed.)* 42, 157–161. <https://doi.org/10.1002/jps.3030420311>.
- Higuchi, W.I., 1967. Diffusional models useful in biopharmaceutics. *J. Pharm. Sci.* 56, 315–324. <https://doi.org/10.1002/jps.2600560302>.
- Hixson, A.W., Crowell, J.H., 1931. Dependence of reaction velocity upon surface agitation. I – Theoretical consideration. *Ind. Eng. Chem.* 23, 923–931.
- Hu, Y., Erxleben, A., Hodnett, B.K., Li, B., McArdle, P., Rasmuson, Å.C., Ryder, A.G., 2013. Solid-state transformations of sulfathiazole polymorphs: The effects of milling and humidity. *Cryst. Growth Des.* 13, 3404–3413. <https://doi.org/10.1021/cg4002779>.
- Huang, Y., Zhang, Q., Wang, J.-R., Lin, K.-L., Mei, X., 2017. Amino acids as co-amorphous excipients for tackling the poor aqueous solubility of valsartan. *Pharm. Dev. Technol.* 22, 69–76. <https://doi.org/10.3109/10837450.2016.1163390doi.org/10.3109/10837450.2016.1163390>.
- Jorgensen, W.L., Duffy, E.M., 2002. Prediction of drug solubility from structure. *Adv. Drug Deliv. Rev.* 54, 355–366. [https://doi.org/10.1016/S0169-409X\(02\)00008-X](https://doi.org/10.1016/S0169-409X(02)00008-X).
- Kishi, H., Hashimoto, Y., 1989. Evaluation of the procedures for the measurement of water solubility and n-octanol/water partition coefficient of chemicals results of a ring test in Japan. *Chemosphere* 18, 1749–1759. [https://doi.org/10.1016/0045-6535\(89\)90459-1](https://doi.org/10.1016/0045-6535(89)90459-1).
- Lipinski, C.A., Lombardo, F., Dominy, B.W., Feeney, P.J., 2012. Experimental and computational approaches to estimate solubility and permeability in drug discovery

- and development settings. *Adv. Drug Deliv. Rev.* 64, 4–17. <https://doi.org/10.1016/j.addr.2012.09.019>.
- Manallack, D.T., 2007. The pKa distribution of drugs: application to drug discovery. *Perspect. Medicin. Chem.* 1, 25–38.
- Morais, I.P.A., Tóth, I.V., Rangel, A.O.S.S., 2006. Turbidimetric and nephelometric flow analysis: concepts and applications. *Spectrosc. Lett.* 39, 547–579. <https://doi.org/10.1080/00387010600824629>.
- Munroe, I., Rasmuson, Å.C., Hodnett, B.K., Croker, D.M., 2012. Relative stabilities of the five polymorphs of sulfathiazole. *Cryst. Growth Des.* 12, 2825–2835. <https://doi.org/10.1021/cg201641g>.
- Noyes, A.A., Whitney, W.R., 1897. The rate of solution of solid substances in their own solutions. *J. Am. Chem. Soc.* 19, 930–934. <https://doi.org/10.1021/ja02086a003>.
- O'Neil, M.J., Smith, A., Heckelmann, P.E., Budavari, S. (Eds.), 2013. *The Merck Index - An encyclopedia of Chemicals, Drugs and Biologicals*, 13th ed. Whitehouse Station, NJ.
- Parasrampur, J., Das Gupta, V., 1990. Development of oral liquid dosage forms of acetazolamide. *J. Pharm. Sci.* 79, 835–836. <https://doi.org/10.1002/jps.2600790919>.
- Prat, D., Wells, A., Hayler, J., Sneddon, H., McElroy, C.R., Abou-Shehata, S., Dunn, P.J., 2016. CHEM21 selection guide of classical- and less classical-solvents. *Green Chem.* 18, 288–296. <https://doi.org/10.1039/c5gc01008j>.
- Shalaeva, M., Kenseth, J., Lombardo, F., Bastin, A., 2008. Measurement of dissociation constants (pKa Values) of organic compounds by multiplexed capillary electrophoresis using aqueous and cosolvent buffers. *J. Pharm. Sci.* 97, 2581–2606. <https://doi.org/10.1002/jps.21287>.
- Stuart, M., Box, K., 2005. Chasing equilibrium: measuring the intrinsic solubility of weak acids and bases. *Anal. Chem.* 77, 983–990. <https://doi.org/10.1021/ac048767n>.
- Stukelj, J., Agopov, M., Yliruusi, J., Strachan, C.J., Svanbäck, S., 2020. Machine-vision-enabled salt dissolution analysis. *Anal. Chem.* 92, 9730–9738. <https://doi.org/10.1021/acs.analchem.0c01068>.
- Stukelj, J., Svanbäck, S., Agopov, M., Löbmann, K., Strachan, C.J., Rades, T., Yliruusi, J., 2019a. Direct measurement of amorphous solubility. *Anal. Chem.* 91, 7411–7417. <https://doi.org/10.1021/acs.analchem.9b01378>.
- Stukelj, J., Svanbäck, S., Kristl, J., Strachan, C.J., Yliruusi, J., 2019b. Image-based investigation: biorelevant solubility of α and γ indomethacin. *Anal. Chem.* 91, 3997–4003. <https://doi.org/10.1021/acs.analchem.8b05290>.
- Sugano, K., Okazaki, A., Sugimoto, S., Tavornvipas, S., Omura, A., Mano, T., 2007. Solubility and dissolution profile assessment in drug discovery. *Drug Metab. Pharmacokinet.* 22, 225–254. <https://doi.org/10.2133/dmpk.22.225>.
- Svanbäck, S., 2016. Toward accurate high-throughput physicochemical profiling using image-based single-particle analysis. University of Helsinki.
- Svanbäck, S., Ehlers, H., Antikainen, O., Yliruusi, J., 2015a. High-speed intrinsic dissolution rate in one minute using the single-particle intrinsic dissolution rate method. *Anal. Chem.* 87, 11058–11064. <https://doi.org/10.1021/acs.analchem.5b03067>.
- Svanbäck, S., Ehlers, H., Antikainen, O., Yliruusi, J., 2015b. On-Chip optofluidic single-particle method for rapid microscale equilibrium solubility screening of biologically active substances. *Anal. Chem.* 87, 5041–5045. <https://doi.org/10.1021/acs.analchem.5b01033>.
- Svanbäck, S., Ehlers, H., Yliruusi, J., 2014. Optical microscopy as a comparative analytical technique for single-particle dissolution studies. *Int. J. Pharm.* 469, 10–16. <https://doi.org/10.1016/j.ijpharm.2014.04.036>.
- Tobiszewski, M., Namieśnik, J., Pena-Pereira, F., 2017. Environmental risk-based ranking of solvents using the combination of a multimedia model and multi-criteria decision analysis. *Green Chem.* 19, 1034–1042. <https://doi.org/10.1039/c6gc03424a>.
- Tosco, P., Rolando, B., Fruttero, R., Henchoz, Y., Martel, S., Carrupt, P.-A., Gasco, A., 2008. Physicochemical profiling of sartans: a detailed study of ionization constants and distribution coefficients. *Helv. Chim. Acta* 91, 468–482. <https://doi.org/10.1002/hlca.200890051>.
- Varshosaz, J., Falamarzian, M., 2001. Drug diffusion mechanism through pH-sensitive hydrophobic/polyelectrolyte hydrogel membranes. *Eur. J. Pharm. Biopharm.* 51, 235–240. [https://doi.org/10.1016/S0939-6411\(01\)00126-6](https://doi.org/10.1016/S0939-6411(01)00126-6).
- Wang, J.R., Wang, X., Lu, L., Mei, X., 2013. Highly crystalline forms of valsartan with superior physicochemical stability. *Cryst. Growth Des.* 13, 3261–3269. <https://doi.org/10.1021/cg400762w>.